

Voltage control in low voltage grids with independent operation of on-load tap changer and distributed photovoltaic inverters

*Original*

Voltage control in low voltage grids with independent operation of on-load tap changer and distributed photovoltaic inverters / Spertino, F.; Ciocia, A.; Mazza, A.; Nobile, M.; Russo, A.; Chicco, G.. - In: ELECTRIC POWER SYSTEMS RESEARCH. - ISSN 0378-7796. - 211:(2022), p. 108187. [10.1016/j.epsr.2022.108187]

*Availability:*

This version is available at: 11583/2969159 since: 2022-06-30T16:59:45Z

*Publisher:*

Elsevier Ltd

*Published*

DOI:10.1016/j.epsr.2022.108187

*Terms of use:*

This article is made available under terms and conditions as specified in the corresponding bibliographic description in the repository

*Publisher copyright*

Elsevier postprint/Author's Accepted Manuscript

© 2022. This manuscript version is made available under the CC-BY-NC-ND 4.0 license  
<http://creativecommons.org/licenses/by-nc-nd/4.0/>. The final authenticated version is available online at:  
<http://dx.doi.org/10.1016/j.epsr.2022.108187>

(Article begins on next page)

# **Voltage Control in Low Voltage Grids with Independent Operation of On-Load Tap Changer and Distributed Photovoltaic Inverters**

Filippo Spertino<sup>1</sup>, Alessandro Ciocia<sup>1</sup>, Andrea Mazza<sup>1</sup>, Marco Nobile<sup>1</sup>, Angela Russo<sup>1</sup>,  
Gianfranco Chicco<sup>1</sup>

<sup>1</sup> Dipartimento Energia “Galileo Ferraris”, Politecnico di Torino,  
Corso Duca degli Abruzzi 24, 10129 Torino, Italy,  
(e-mail: {filippo.spertino, alessandro.ciocia, andrea.mazza, angela.russo,  
gianfranco.chicco} @polito.it, marco.nobile@studenti.polito.it)

Corresponding author:

Alessandro Ciocia Dipartimento Energia “Galileo Ferraris”

Corso Duca degli Abruzzi 24, I-10129 Torino, Italy

e-mail [alessandro.ciocia@polito.it](mailto:alessandro.ciocia@polito.it)

**Abstract:** This paper aims to find the optimal setups of voltage control devices in different configurations of Low Voltage (LV) grids with strong PhotoVoltaic (PV) diffusion by performing dedicated simulations. Distributed PV inverters and On-Load Tap Changer (OLTC) are simulated without considering their coordination, to avoid large investments in new communication infrastructures. Thus, each device independently works to decrease voltage deviations in the respective grid connection point. PV generation and consumption profiles are measured and used in two simulated LV grids, connected to the Medium Voltage (MV) grid by a MV/LV transformer with rated powers of 400 and 250 kVA, respectively. The calculation of the optimal devices setups is addressed as a multi-objective problem, considering objectives of voltage quality, grid losses, and OLTC lifespan increase. Multiple simulations are performed by varying the setup of the voltage controls, and considering different positioning and sizes of the generators. In the hardest case, the ratio between the maximum PV power generation and the maximum load in the whole grid is  $\approx 70\%$ . Pareto analysis is carried out to find the non-dominated solutions and TOPSIS is applied to rank the solutions. Finally, a sensitivity analysis is performed by changing the weights attributed to each objective function.

**Keywords:** Voltage control, low voltage grid, photovoltaic system, reactive power, on-load tap changer, Pareto front, sensitivity analysis, TOPSIS method.

## **1. Introduction**

In the last decades, the increase of distributed generation in Low Voltage (LV) distribution grids lowered the energy production dependence from the centralized power plants. The number of distributed renewable energy systems, mainly PhotoVoltaic (PV) generators, is increasing, supporting the reduction of greenhouse gas emissions. Due to the fluctuations of solar irradiance, PV generation is highly variable and may lead to voltage fluctuations, reverse power

flows and power quality issues [1][2].

A general method to reduce voltage violations in LV grids calls for grid investments from the Medium Voltage (MV) connection point, e.g., with replacement of the MV/LV transformer and/or the reduction of the cable impedances [3]. However, these solutions are costly and only partially effective and hence, with larger and larger share of distributed generation (mainly PV systems), the LV grid operation will require more advanced voltage control techniques.

In the literature, many articles describe various methods to perform voltage control. It is clearly established that both centralized and local voltage controls have to be simultaneously present to ensure more options for effective voltage control. For centralized control, one of these methods involves the operation of the On-Load Tap Changer (OLTC), which modifies the tap position of the transformer to reach the voltage target. This device is mainly used on the High Voltage (HV) side of the HV/MV transformers, for controlling voltage in the MV grid. However, in recent years, it is also being used in LV grids [4]. For example, the unbalanced MV electrical grid (IEEE-123 nodes), characterized by a significant presence of PV generators, is analyzed in [5]. The control is carried out by OLTC and PV inverters that provide inductive or capacitive reactive power. In some cases, the voltage variation at the node with OLTC can cause voltage violations, especially in the nodes with high generation and low load. In this case, distributed control is fundamental because it acts locally at the node where the violation occurs [3]. It is noted that in [5] there is a communication system between inverters and the OLTC. With respect to [5], the MV grid analyzed in [6] is divided into several zones, each one equipped with an autotransformer and/or other devices, such as Capacitor Banks (CB), static reactive power compensators (STATCOM) and/or PV inverters. The logic for the reactive and active power control aims to minimize the number of tap changes of the OLTC by regulating more with other devices. Nevertheless, the study is based on the use of a communication system between the devices to perform real-time coordinate voltage control.

The IEEE 123-node MV grid is used in [7], with voltage control devices, such as Static Var Compensator (SVC) and OLTC, which communicate to improve voltages. The goal is to minimize different objective functions (total grid losses, number of tap changes, and SVC wear). To solve this multi-objective problem, a weight is assigned to each objective function. By changing the weights, the performance of each different control is discussed. In [8], the voltage is regulated by inverters that provide inductive or capacitive reactive power to stabilize the voltage at the Point of Common Coupling (PCC). They interact via a real-time communication system. Proportional Integral (PI) regulators are used to provide closed-loop voltage control between the grid and PV systems and make the control faster and more efficient. In [9], the voltage is regulated via PV inverters providing reactive power; PI regulators are used for the control logic, to decrease the voltage deviation and try keeping the losses low. In this case, centralized devices are not considered.

In [10], a mixed control is performed, with a coordination system among distributed and centralized devices. In particular, the grid is divided into several zones, each consisting of a certain number of cascaded devices. A ZIP-type load model is used, and the volt-var optimization method allows to reduce the number of tap changes. Three objective functions are defined, related to the number of tap changes, the Step Voltage Regulator (SVR) wear, and the generated active power. The first two objective functions are minimized, while the third one is maximized. From the results obtained, a decrease of the voltage deviation is due to the number of tap changes executed. Moreover, storage systems are used to improve the control performance. The MV grid in [11] is divided into zones, each of them is equipped with control devices (inverter, OLTC, CB and SVR). With respect to other papers, there is no communication system, every device is independent of others and regulates only the voltage in its PCC, and the distributed inverters use reactive power to control voltage.

Another method to control voltage in LV grids with high PV generation is the Active Power

Curtailment (APC) [12]. It consists of the reduction of active power generated to reduce the voltage at the PCC. In particular, there are two different approaches: in the first one, all inverters have the same reduction logic; in the second one, the setups are different. From the results obtained in [12], in the second approach a lower voltage deviation is obtained than in the first one, but with more Joule losses. The APC method is more efficient if there is a coordination between devices [13]. In the absence of a communication system, it is more convenient to regulate by providing only reactive power. In this way, the active power does not change, and the energy produced is maximized, as described in [14] and [15]. In these two works, the control is performed only by PV inverters that provide inductive or capacitive reactive power. The reactive and APC method can be combined, as in [12] and [16].

Furthermore, Battery Energy Storage Systems (BESS) can be used to increase the control effectiveness [16][17]. In [18] and [19], BESS and PV inverters are used to control voltage. In particular, in [20] each PV system is equipped with BESS which store energy only when the active power generated is greater than a threshold. This solution leads to a reduction of the voltage deviation. The work [19] studies how the control performance changes according to the characteristics of the grid. In urban grids characterized by relatively short distribution lines and non-negligible transformer parameters, with low R/X ratio (about 1), the reactive power provided by PV inverters is sufficient to adjust the voltage effectively. Instead, in rural grids characterized by longer distribution lines and higher R/X ratio (about 4÷5), it is advisable to regulate the voltage using PV inverters and BESS. The drawbacks of these last two works are the high cost of BESS and the absence of centralized devices. A solution that considers the costs in the optimization of LV distribution networks with OLTC, PV inverters and BESS is proposed in [20].

With respect to the analyzed papers, the present work does not consider coordination systems, and each device regulates the voltage independently and for each phase. Moreover, to maximize

the use of renewable sources, it is not considered the possibility to reduce the active power generated to mitigate the voltage issues. No BESS is included, to avoid the related costs. The present paper improves the work in [21], by describing in detail a more advanced procedure to perform the voltage control using centralized and distributed devices. In addition, Pareto analysis and TOPSIS are used to calculate the optimal setups of all the control devices. A sensitivity analysis is added to study the results variation as a function of the weights of the multi-objective problem. Finally, the whole procedure is applied to two different LV grids and results are discussed.

The next sections of this paper are organized as follows. Section 2 describes the voltage control methods. Section 3 describes the proposed procedure to find the optimal setups of the PV inverters and OLTC for the voltage control. Section 4 presents the case studies. Section 5 shows the simulation results. The last Section contains the conclusions.

## **2. Simulation of voltage control solutions**

The various aspects of simulating the voltage control by considering centralized and distributed Voltage Control Devices (VCDs) are addressed below. Section 2.1 describes the procedure used to simulate the operation of a LV grid with VCDs, i.e., an OLTC and distributed PV inverters. After the general description of the whole procedure, Section 2.2 presents the details about the proposed logic for the voltage control performed by distributed PV inverters, that is, based on voltage criteria, voltage limits, and the logic to reach the optimal reactive power. Finally, Section 2.3 presents the logic used to perform voltage control by OLTC, showing the details of the procedure for the simulation of the OLTC operation and presenting a simple example of the effect of changing the setup parameters of the OLTC.

### *2.1 Voltage control by centralized and distributed devices*

Fig. 1 shows the flowchart of the whole procedure to calculate the power flows and simulate the voltage control for both centralized and distributed VCDs. Assuming steady state condition, the procedure is repeated for each time step, which in the present work is 1 minute. The time step of 1 min is typical for steady-state simulations for voltage control analysis [22][23][24]. It permits to avoid the detailed modelling of dynamic processes of the equipment involved in the voltage control. For example, in case of the OLTC equipped with transition resistors, the transition between the resistors causes the current to vary during the switching process. In particular, winding inductance, contact resistance and contact movement, interruptions and arcing may affect the current amplitude [25][26]. The total operation time of an OLTC is between few seconds to tens of seconds, depending on the respective design [27]. On these bases, the time step of 1 min is sufficiently long to avoid the need of representing the dynamics of the tap changers, which are faster.

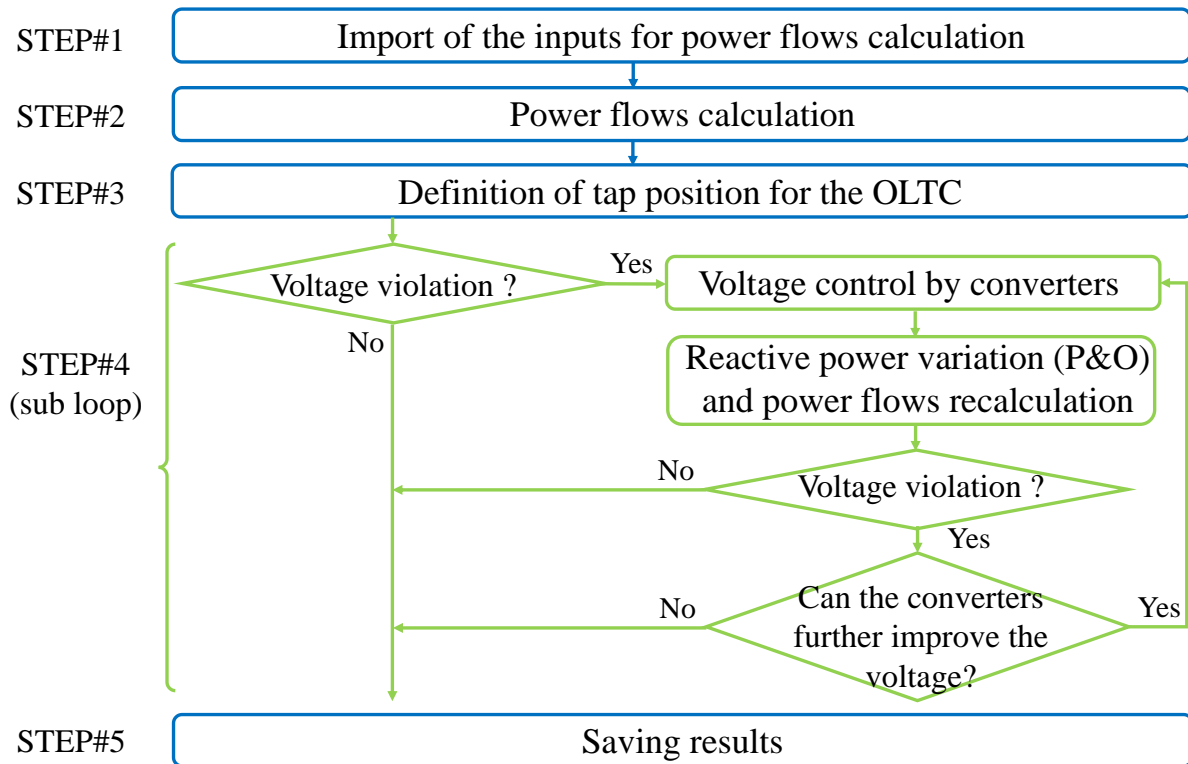


Fig. 1. Procedure for power flows calculation and voltage control performed for each 1-min time step of the simulation.

The procedure is composed of the following steps:



- STEP#1: the inputs for power flow calculation (e.g., grid data, generation and load profiles, capability curves, parameters of the controllers, voltage limits) are imported. From the second minute onwards, the inputs include the OLTC tap position, and the updated parameters of the OLTC proportional-integral control.
- STEP#2: a first power flow calculation is performed for time step  $t$  without change in the voltage control, with respect to the previous time step  $t-1$ . The Backward Forward Sweep (BFS) method is performed in the three-phase unbalanced LV grid. The equations to calculate the voltages and currents are indicated in [28]. The detailed procedure for power flow calculation and voltage control works according to [29].
- STEP#3: the tap position of the OLTC is calculated, according to the PI control described in Section 2.3.
- STEP#4: it consists of a sub-loop that can be run several times for each time step. A check of voltage violation for each node of the grid with a PV inverter is performed. In case of violation, the power flows are recalculated with the BFS by considering new reactive power quantities according to a logic which looks for the best quantity of reactive power to inject/absorb. The PV inverter continues to regulate, and simulations are repeated until there is no voltage violation, and not even one inverter can further improve the voltage (i.e., all control criteria are satisfied). The criteria that define if the inverters cannot further improve the voltage resulting in the exit from this sub-loop, and the logic to regulate reactive power, are described in Section 2.2.
- STEP#5: in absence of voltage violations or control possibility, the procedure exits from the loop, and data are saved.

The previously described procedure is repeated for each time step. At the end of the simulations, the losses and voltage indicators are calculated to compare the results obtained for different setups of the devices. All the calculations in this paper are performed by a Matlab<sup>®</sup> code written

183 by the authors.

## 184 2.2 Voltage control by distributed PV inverters

185 In case of voltage violations, the PV inverters provide inductive or capacitive reactive power to  
186 keep the voltage within the limits. In different countries, the standards require that the PV  
187 inverters can provide reactive power to support the grid operation. For example, the Italian  
188 standard CEI 0-21 used for LV grids [30] defines two capability curves depending on the rated  
189 active power  $P_{\text{rated}}$  of the PV system. The feasible operation region for the active and reactive  
190 power generated is located inside the corresponding capability curve. The numerical threshold  
191 on  $P_{\text{rated}}$  is determined by considering the rated voltage  $V_{\text{rated}} = 400$  V, the rated current  $I_{\text{rated}} =$   
192 16 A, and the power factor  $PF = 1$ , so that  $P_{\text{rated}} = \sqrt{3} V_{\text{rated}} I_{\text{rated}} PF_{\text{ref}} = 11.08$  kW. The  
193 formulation of the maximum power for the two capability curves is based on the reference  
194 power factor  $PF_{\text{ref}} = 0.9$ :

- 195 1) If  $P_{\text{rated}} \leq 11.08$  kW, the maximum reactive power depends on the active power  
196 generated  $P$ , as  $Q_{\text{max}}(P) = P \operatorname{tg}(\arccos(PF_{\text{ref}}))$ , so that the power factor never decreases  
197 below the limit  $PF_{\text{ref}}$  [30].
- 198 2) If  $P_{\text{rated}} > 11.08$  kW, the maximum reactive power  $Q_{\text{max}}$  is constant and is determined as  
199  $Q_{\text{max}} = P_{\text{rated}} \operatorname{tg}(\arccos(PF_{\text{ref}})) = 0.484 P_{\text{rated}}$ , independently of the active power generated.

200 In both cases, the capability curves are symmetrical with respect to the reactive power, so that  
201 the minimum reactive power is  $Q_{\text{min}}(P) = -Q_{\text{max}}(P)$  in the first case and  $Q_{\text{min}} = -Q_{\text{max}}$  in the  
202 second case.

203 As previously mentioned, in the present work there is no communication system, and each PV  
204 inverter manages reactive power independently of the others [31][32]. This logic is created to  
205 simplify the real implementation of Voltage Control Devices (VCDs) in actual grids. In fact,  
206 the whole procedure is based on the comparison between the voltage measured by the device

in its connection point and voltage limits. Each VCD does not require communication, because each device works autonomously, without cooperating with a centralized VCD (e.g., an OLTC) or other distributed VCDs. In a real implementation, the devices do not need to know advanced information about the grid, such as the number of nodes, the number of lines and the related impedances, etc. In fact, the VCDs operate only on the basis on the local information (the power flow is not calculated by VCDs). As a result, the VCDs logics do not change in case of the installation of additional distributed generation, or in case of changes in the grid configuration, which modify the impedance seen from the point of connection of the VCD.

#### *2.2.1 Perturb & Observe technique for voltage control*

The control of one device can improve voltage in its node and can affect the other nodes. In this paper, the logic used to calculate the best reactive power quantity is based on the Perturb & Observe (P&O) technique. It is a logic widely used to obtain the maximum power point of the DC side of the PV inverters [33]. The principle of operation of the original P&O is briefly described with the following example. A PV inverter is working at a DC voltage power level defined by environmental conditions (irradiance and temperature). To reach the maximum output, the PV inverter increases the DC voltage of the PV modules and measures the new DC power production. If the production increases, the increase is repeated until there is no significant improvement of the power output. On the contrary, if the change in the DC voltage leads to a decrease of the output power, the procedure will be repeated in the opposite direction, i.e., by reducing the DC voltage [34]. In the present work, a similar P&O is used. The reactive power is changed to reduce the voltage deviation, i.e., the difference between the voltage measured at point of connection of the PV inverter with the grid and the reference voltage equal to 1 per unit (p.u.). In case of voltage violation, reactive power is added (capacitive for undervoltage, inductive for overvoltage): the electronic circuits in the PV inverter increase or decrease (with its sign) the phase angle between current and voltage to change the reactive

power injected or absorbed. If the voltage violation is reduced but not solved, the inverter increases its reactive power. If the change in reactive power does not lead to a voltage improvement, the control ends to avoid an unnecessary increase of the total Joule losses  $L_{tot}$ .

### 2.2.2 Voltage limits

The setup of the voltage control is changed by modifying the limits shown in Fig. 2 [29]:

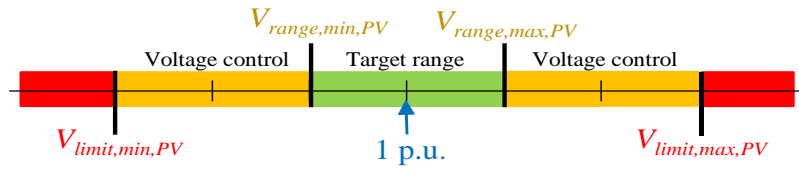


Fig. 2. Voltage limits for the PV inverters contributing to voltage control

The inverters do not provide reactive power when the voltage is included in the range  $V_{range,min,PV} - V_{range,max,PV}$ . If the voltage is between  $V_{range,min,PV}$  and  $V_{limit,min,PV}$  or between  $V_{range,max,PV}$  and  $V_{limit,max,PV}$ , the inverter works to correct the voltage violation. In case of overvoltage ( $V_i > V_{range,max,PV}$ ), the inverters provide inductive reactive power to reduce the voltage. The proposed voltage control could work also in case of larger violations, i.e., the red areas in Fig. 2 corresponding to a voltage lower than  $V_{limit,min,PV}$  or higher than  $V_{limit,max,PV}$ . Nevertheless, in these cases, the voltage control is stopped to avoid interactions with other logics included in the real applications. In fact, according to different grid codes [30][35], the inverters have other tasks to perform: grid codes require the PV systems to provide low voltage ride-through (LVRT) capability, i.e., the ability to withstand the abnormal voltage and remain grid-connected in the event of grid failures [36]. The timing of LVRT is about hundreds of milliseconds, very fast with respect to the time steps considered in this paper, and if the voltage remains outside the limits for a longer period there is the disconnection of the PV inverter from the grid, operated by the protection systems. As such, voltage control is active only inside the voltage control ranges indicated in Fig. 2. A detailed discussion on LVRT capability is out of scope for this paper.

### 2.2.3 Voltage control criteria

In the sub-loop described in the previous subparagraph, corresponding to STEP#4 in Fig. 1, at every iteration, each inverter has to respect a set of criteria to manage its reactive power. These criteria are used to guarantee the correct operation of the inverters and avoid useless reactive power in the grid. The individual inverters are not influenced by the criteria applied to the other devices and can be stopped in controlling voltage during an iteration, and restart in the next iteration. For example, let us suppose that, at the first iteration, an inverter in a generic node#A does not provide reactive power, because there is no violation in its PCC, but an increase in the reactive power injection in other nodes leads to a violation in node#A. Thus, the inverter in node#A will work to adjust its voltage until all its criteria are satisfied.

The criteria are:

- *Usefulness criterion*: if the voltage difference  $V_i^{(k)} - V_i^{(k-1)}$  between two iterations ( $k$  and  $k-1$ ) is less than a threshold ( $V_i^{(k)} - V_i^{(k-1)} < \varepsilon$ ), the inverter stops the control to avoid a useless increase of the losses  $L_{tot}$ . A low value of  $\varepsilon$  makes the inverters to use all their reactive power. This threshold permits the inverters, that cannot significantly contribute to the improvement of voltage profiles, to exit from the loop.
- *Consistency criterion*: there is an inconsistency if the inverter provides inductive power and its PCC voltage increases, or if it provides capacitive power and the voltage decreases. The reason is that in these cases the control of the voltage is useless; voltage variation is dominated by other devices in the grid (for example another PV generator with a much higher power in a close node). In these cases, the inverter stops the reactive power variation.
- *Saturation criterion*: when the inverter exceeds the maximum reactive power according to its capability curve, it saturates and stops the control. Obviously, if a reactive power reduction is required, the inverter applies it.

### 2.3 Voltage control performed by OLTC

Centralized voltage control by On Load Tap Changer (OLTC) is based on PI control [29]. By changing the tap, the goal of the control is to keep the voltage at the LV side of the transformer as close as possible to the target voltage  $V_{\text{target}}$ . A key parameter of this control is the over-under voltage counter  $\alpha_{\text{OLTC}}(t)$ . The procedure to control the OLTC is shown in the flowchart in Fig. 3:

- STEP# $\alpha$ : the data from the previous time step  $t-1$  are imported. They are the updated voltage counter  $\alpha_{\text{OLTC}}(t-1)$ , and the tap position to be used in time step  $t$ .
- STEP# $\beta$ : simulations are performed for time step  $t$ . From all the results (currents, voltages, power flows, losses, etc.), it is calculated the deviation  $\Delta V_{\text{OLTC}}$  between the simulated voltage at the LV side of the transformer  $V_{\text{OLTC}}$  and the target  $V_{\text{target}}$ .
- STEP# $\gamma$ : the voltage violation at the LV side of transformer is verified. In fact, to avoid excessive tap changes, the OLTC control changes if the voltage is outside or inside the deadband  $\pm DB$ .
- STEP# $\delta 1$ : in case of voltage violation (i.e.,  $|\Delta V_{\text{OLTC}}| > DB$ ) voltage counter  $\alpha_{\text{OLTC}}(t)$  is updated by adding or subtracting the quantity  $\alpha_{\text{OLTC},\Delta t}$ , as defined in (1):

$$\alpha_{\text{OLTC}}(t) = \alpha_{\text{OLTC}}(t-1) \pm \alpha_{\text{OLTC},\Delta t}(t-1) \quad (1)$$

The increment  $\alpha_{\text{OLTC},\Delta t}$  is proportional to the absolute value of  $\Delta V_{\text{OLTC}}$ , as shown in (2):

$$\alpha_{\text{OLTC},\Delta t}(t) = \frac{2 \cdot (|\Delta V_{\text{OLTC}}|)}{t_{\text{adm}} \cdot DB} \Delta t = \frac{2 \cdot (|V_{\text{OLTC}}(t) - V_{\text{bus,BT}}|)}{t_{\text{adm}} \cdot DB} \Delta t \quad (2)$$

where  $\alpha_{\text{OLTC},\Delta t}$  is inversely proportional to  $DB$  and depends on the admitted voltage violation time  $t_{\text{adm}}$  (whose effect will be shown in Fig.4). In the present work, the voltage deadband  $DB$  is equal to half a tap ( $DB = \Delta V_{\text{tap}}/2$ ). If the parameter  $\alpha_{\text{OLTC}}(t)$  exceeds the limits  $\pm 1$ , it is saturated at  $\pm 1$ .

- STEP# $\delta 2$ : in case of no voltage violation ( $|\Delta V| < DB$ ),  $\alpha_{\text{OLTC}}(t)$  is partially reset. This partial reset is necessary to avoid unnecessary tap changes due to violations occurred

much earlier. For example, a temporary overvoltage occurred in the early morning should not lead to a tap change in the late afternoon. Thus, at each step without voltage violation, the parameter  $\alpha_{\text{reset}}$  (over-under voltage parameter) is used to decrease the value of  $\alpha_{\text{OLTC}}(t)$  according to (3):

$$\alpha_{\text{OLTC}}(t) = \alpha_{\text{OLTC}}(t-1) \pm 1/\alpha_{\text{reset}} \quad (3)$$

The parameter  $\alpha_{\text{reset}}$  represents the time (in minutes) necessary to reset the counter  $\alpha_{\text{OLTC}}(t)$ . In fact, after a number of time steps with no violations equal to  $\Delta\alpha_{\text{OLTC}}$ , the counter  $\alpha_{\text{OLTC}}(t)$  is restored back to zero.

- STEP# $\epsilon$ : if  $|\alpha_{\text{OLTC}}(t-1)|=1$ , the tap position changes at the beginning of the next time step  $t$ . If  $\alpha_{\text{OLTC}}(t)=1$ , the tap increases  $\text{tap}(t) = \text{tap}(t-1)+1$  for a lower voltage; if  $\alpha_{\text{OLTC}}(t)=-1$ , the tap decreases to obtain a higher voltage.
- STEP# $\zeta$ : in the last step, the updated value of  $\alpha_{\text{OLTC},\Delta t}$ , and the updated tap position to be used in the next simulation, are saved. It is noteworthy that, after a tap change, a minimum time  $t_{\text{min,two,taps}}$  is waited before permitting another one to avoid fast tap oscillations.

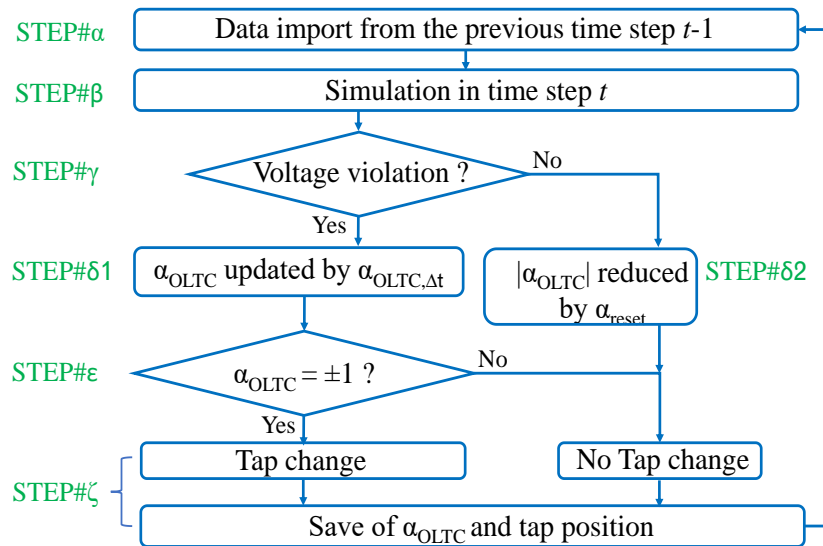


Fig. 3. Procedure for the control of the OLTC.

### 2.3.1 Example of the effect of the change of the setup parameters for the OLTC

As mentioned in STEP# $\delta 1$ , a key parameter to control the OLTC is the time  $t_{\text{adm}}$ ; it changes the

slew rate of the device limiting the number of tap changes  $N_{\text{tap}}$ . In fact, according to (2),  $\alpha_{\text{OLTC},\Delta t}$  and  $t_{\text{adm}}$  are inversely proportional. In conclusion, a high value of  $t_{\text{adm}}$  leads to a lower slew rate of the OLTC. This is confirmed by the example presented in Fig. 4, in which three simulations are presented. They are characterized by different parameters of proportional-integral control: in case (a), the parameters are  $t_{\text{min,two,taps}}=30$  min,  $t_{\text{adm}}=20$  min,  $\alpha_{\text{reset}}=30$ . In case (b) the setup is  $t_{\text{min,two,taps}}=30$  min,  $t_{\text{adm}}=5$  min and  $\alpha_{\text{reset}}=40$ ; in case (c) the setup is  $t_{\text{min,two,taps}}=10$  min,  $t_{\text{adm}}=5$  min and  $\alpha_{\text{reset}}=10$ . For the sake of clarity, only the first phase is represented in Fig. 4. In case (a), during the whole day, the OLTC executes 2 tap changes, whereas in case (b) there are 4 tap changes. In the last case, the number of tap changes is the highest (six) because all the parameters are the lowest (have the lowest values). In cases (b) and (c), the OLTC is very sensitive due to the low  $t_{\text{adm}}$ . The small value of  $t_{\text{min,two,taps}}$  in case (c) permits to perform more tap changes in a reduced time frame.

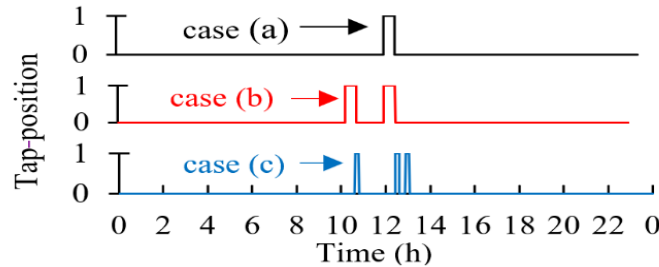


Fig. 4. Tap position by varying  $t_{\text{min,two,taps}}$ ,  $t_{\text{adm}}$  and  $\alpha_{\text{reset}}$ .

### 3. Optimal Setups of Voltage Control Devices

The decision variables considered in this analysis are the parameters of the VCDs. The effects of these parameters on the voltage profiles of the LV grids under study, as well as the Joule losses in the lines and the number of tap changes of the OLTC, are taken into account and play a fundamental role in the optimization process. Section 3.1 describes the indicator used to evaluate the voltage deviations in the whole LV grid. Section 3.2 presents the complete lists of the parameters used for setting up the VCDs; these are the inputs parameters that are changed



in each simulation scenario. The scenarios are created to study the effect of the change in the inputs parameters on the optimization results. Finally, Section 3.3 presents the procedure to find the optimal setups.

### 3.1 Voltage indicators

The calculation of voltage indicators allows to evaluate the effectiveness of each type of voltage control. Among all the possible voltage indicators useful to calculate the quality of the voltage profiles, the most important used in the present work is the Voltage Deviations with Energy Flows (*VDEF*) [29]. It counts the sum of the squares of voltage deviations (with respect to a reference value  $V_{ref}$ ) in each node  $k$  of the grid and at each time step  $t$ . Each deviation is multiplied by the energy  $E_{k,t}$  to give more importance to the nodes and time steps in which the consumption is higher [37]. This sum is divided by the total energy consumed in the grid during the simulated period:

$$VDEF = \frac{\sum_{t=1}^M \sum_{k=1}^{N_{nodes}} (V_{k,t} - V_{ref})^2 \cdot E_{k,t}}{\sum_{t=1}^M \sum_{k=1}^{N_{nodes}} E_{k,t}} \quad (4)$$

with  $M$  indicating the maximum number of time steps composing the timeframe  $T$ .

### 3.2 Input parameters of voltage control devices

According to [21], [29], [38], and this work, the variation of the input parameters (setup) of distributed PV inverters affects the three objective functions  $L_{tot}$ ,  $N_{tap}$  and *VDEF* as follows:

- $V_{limit,max,PV}$ : a reduction of this parameter leads to a restriction of the band delimited by  $V_{range,max,PV}$  and  $V_{limit,max,PV}$ , and the decrease of the *VDEF* of the grid. However,  $L_{tot}$  increases due to the inductive power supplied to reduce the overvoltage.
- $V_{range,max,PV}$ : a reduction of this parameter leads to a restriction of the target range delimited by  $V_{range,min,PV}$  and  $V_{range,max,PV}$ . In this case, the PV inverters provide more inductive power to decrease the *VDEF* and to stabilize the voltage below the limit.

- $V_{\text{range,min,PV}}$ : an increase of this parameter leads to a reduction of the target range between  $V_{\text{range,min,PV}}$  and  $V_{\text{range,max,PV}}$ . In this way,  $L_{\text{tot}}$  increases, but the  $VDEF$  decreases because the inverters provide more capacitive power to stabilize the voltage above the limit.
- $V_{\text{limit,min,PV}}$ : an increase of this limit leads to a reduction of  $VDEF$ , but  $L_{\text{tot}}$  can increase if the inverters provide higher capacitive power to stabilize the voltage above the limit.

The effects of the variation of the setup parameters of the OLTC are described in the following list:

- $V_{\text{target}}$ : it is the voltage goal for the OLTC. The variation of this parameter leads to a voltage variation in all the grid.
- $t_{\text{adm}}$ : a reduction of this parameter leads to an increase of  $\alpha_{\text{OLTC},\Delta t}$ ; thus, the number of tap changes  $N_{\text{tap}}$  increases leading to a reduction of  $VDEF$ .
- $t_{\text{min,two,taps}}$ : an increase of this parameter leads to a reduction of  $N_{\text{tap}}$  because the tap changer cannot work for a longer time after a step. Thus, the  $VDEF$  increases because of a reduced operation of the OLTC.
- $\alpha_{\text{reset}}$ : a high value of this parameter implies a lower slew rate of the OLTC; thus, a reduction of the  $N_{\text{tap}}$  and an increase of  $VDEF$ .

All the above parameters differ for every scenario and are randomly changed inside specific ranges. For the voltage limits of inverters,  $V_{\text{limit,min,PV}} > 0.9$  and  $V_{\text{limit,max,PV}} < 1.1$ . According to Fig. 2,  $V_{\text{range,max,PV}}$  and  $V_{\text{range,max,PV}}$  lie within those limits.

For the OLTC,  $V_{\text{target}}$  is close to unity,  $t_{\text{adm}}$  and  $t_{\text{min,two,taps}}$  are in the range  $1 \div 30$  min, and  $\alpha_{\text{reset}}$  varies between 1 and 30.

### 3.3 Calculation of the optimal setups for voltage control

Fig. 5 shows the proposed procedure to study and compare different setups of the voltage control devices by solving the multi-objective problem.

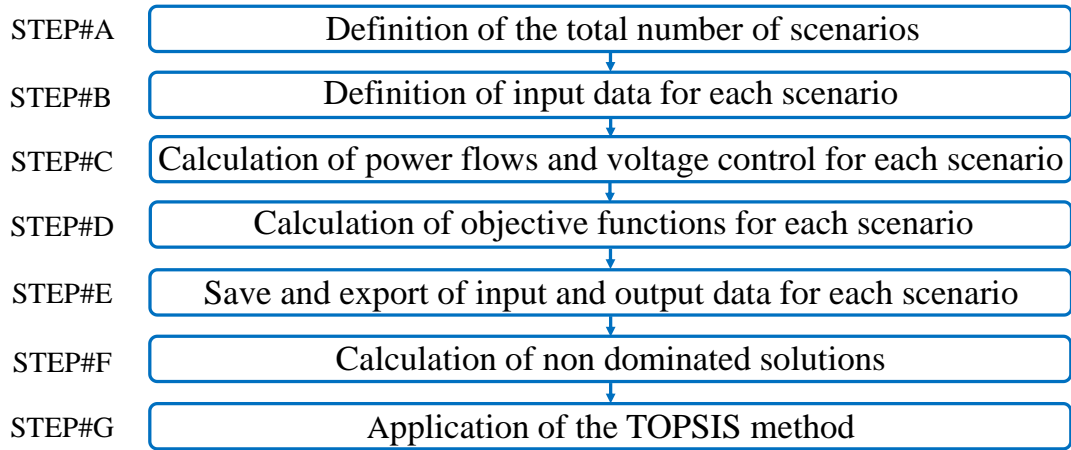


Fig. 5. Procedure for the study of optimal setups of voltage control devices.

- STEP#A: the procedure starts with the selection of the total number of scenarios to be analyzed. It is an information that affects the simulation time.
- STEP#B: the inputs to be changed in each scenario are selected. They are the setup of the voltage control devices, e.g., the voltage limits of the capability curves of PV inverters and the parameters of the PI control. The complete list of the setup parameters was presented in the previous Section 3.2.
- STEP#C: the power flows are calculated, and the voltage control is performed. Each scenario has a different simulation performed according to the methodology explained in Section 2 for a timeframe  $T$  with time step  $t$ .
- STEP#D: the objective functions are calculated to perform the optimization. In the proposed procedure, the objective functions are the Joule losses for the whole grid  $L_{tot}$ , the number of tap changes  $N_{tap}$ , and the voltage indicator  $VDEF$ .
- STEP#E: all input and output data of each scenario are saved and organized for the next Pareto analysis.
- STEP#F: within all the sets of results, those that belong to the Pareto front are identified. They represent the non-dominated solutions for which there is no objective function that is simultaneously better for all the analyzed objective functions.

- STEP#G: the TOPSIS method [39] is applied to determine the ranking of the best solutions that belong to the Pareto front. It is noted that the results obtained with TOPSIS method depend on the weight assigned to each objective function. Moreover, the sum of all weights must be 1.

## 4. Case Studies and Grid Configurations

The various aspects that refer to the preparation of the data for running the optimization procedure are described below. Section 4.1 contains the description of the two grids under analysis. Section 4.2 provides information about the measurement of generation and load profiles used as inputs for the simulations. Section 4.3 shows how the combination of the two grids and the measured profiles leads to the creation of different configurations. The resulting configurations correspond to the two grids considered, with renewable energy generators positioned in different nodes in the grid and with different nominal sizes.

### 4.1 Description of the case studies

The simulations are performed on two LV grids:

1. Grid#1 (20 lines, 21 nodes); contains a three-phase transformer (20 kV/400 V, rated power  $S_{\text{rated,tr}} = 400$  kVA, rated current  $I_n = 570$  A, short-circuit impedance  $Z_{\text{sc}} = 24$  m $\Omega$  and short circuit power losses at 75°C  $P_{\text{sc},75^\circ\text{C}} = 4.7$  kW).
2. Grid#2 (18 lines, 19 nodes); contains a three-phase transformer (20 kV/400 V, rated power  $S_{\text{rated,tr}} = 250$  kVA, rated current  $I_n = 361$  A, short-circuit impedance  $Z_{\text{sc}} \cong 38$  m $\Omega$  and short circuit power losses at 75°C  $P_{\text{sc},75^\circ\text{C}} = 3.4$  kW).

In both grids, the slack node #0 is the MV bus of the MV/LV substation. In all the lines, the resistive component of the cables prevails over the inductive one. The LV grids have grounded neutral and lines with three-pole underground cables, except for the overhead cables in

proximity of the transformer. The structure of each grid is shown in [29]. The transformer is represented by the pi-model, neglecting the iron losses. The series impedance is calculated starting from the transformer datasheets. The tap changer has a voltage step of 1.25% of the nominal value and seven tap positions  $(-3, \dots, 0, \dots, +3)$  corresponding to LV-side voltage changing in the range 0.9625 – 1.0375 p.u. when the transformer is supplied at nominal primary voltage.

#### 4.2 Load and generation profiles

Load and generation profiles have been measured using the Data Acquisition System (DAS) described in [40] and characterized by relative uncertainties equal to about 1%. The generation profiles consist of active power values measured during a week in September, which adequately represent an average generation along the year. These measured generation profiles are used as a reference sample: the generation in each node is recreated by amplifying the measured profiles without considering partial shading effects on the PV modules. On the contrary, the reactive power profiles from the PV inverters are simulated according to the voltage control described in the presented work. Regarding the load profiles, they are active and reactive power absorptions of the aggregation of apartments and offices.

#### 4.3 Grid configurations

In Grid#1, the ratio  $\theta_{PV}$  between the maximum power produced by all the PV generators and the maximum load in the whole grid is  $\theta_{PV,grid1} \approx 46\%$  due to an overall PV nominal power at AC side of 250 kVA. In Grid#2, this ratio is  $\theta_{PV,grid2} \approx 50\%$  due to an overall PV nominal power of 126 kVA. It is worth noting that the load and generation power peaks used to calculate these ratios are not simultaneous. For these two reference grid configurations, simulations are carried out by changing the position of load and generators or by increasing  $\theta_{PV}$ . The increase of  $\theta_{PV}$  is obtained selecting generation profiles with higher production. For each configuration listed in

Table 1, the procedure for the study of optimal setups (Fig. 5) is applied and results are discussed in the next subparagraphs.

**Table 1. Grid Configurations**

Grid	Configuration	Description
1	CONF#1	Reference configuration for Grid#1
	CONF#2	Different positions of loads and generators
	CONF#3	Higher PV production peak - $\theta_{PV,grid1} \approx 55\%$
2	CONF#4	Reference configuration for Grid#2
	CONF#5	Different positions of loads and generators
	CONF#6	Higher PV production peak - $\theta_{PV,grid2} \approx 70\%$

## 5. Simulation Results

The results of the simulations performed are shown below. Section 5.1 presents examples of daily voltage profiles obtained by controlling the PV inverters and the OLTC, following the logics and procedures described in the previous sections. These examples are useful to better understand the effects of the different voltage controls. For this purpose, the proposed graphs show the controlled voltage profiles with respect to the same cases in which control is absent. After the examples, Section 5.2 and Section 5.3 present the aggregated results of the simulation of 6000 scenarios, each one with a different setup of the voltage controls. To compare the results, a TOPSIS solutions ranking is applied, and the best scenarios are found from the ranking. Finally, a sensitivity analysis is performed to analyze how the the ranking of the solutions changes by using different weights for the objective functions.

### 5.1 Examples of simulated voltage profiles obtained by controlling PV inverters and the OLTC

All types of voltage control are performed for a week with 1-minute time step. Fig. 6 shows a daily example of voltage profiles calculated without voltage control (CONF#1, day#1, node #18). In the figure, this profile can be compared with the one obtained in case of reactive power control from the PV inverter. Profiles refer to node #18, that is, the one with the highest impedance. The horizontal lines are the limits for the voltage control of the inverter. If the

voltage is higher than  $V_{\text{range,max,PV}}$ , the inverter provides inductive reactive power to stabilize the voltage below the limit border. In this example, between hours 12:00 and 14:00, the voltage is higher than the limit border due to the peak of PV production; thus, the inverter provides inductive power (peak  $\approx 15$  kvar). No capacitive power is supplied because the voltage is never below  $V_{\text{range,min,PV}}$ . The active and reactive power profiles related to Fig. 6 are shown in Fig. 7. For the sake of clarity, all these profiles refer to the first phase of the unbalanced three phase system.

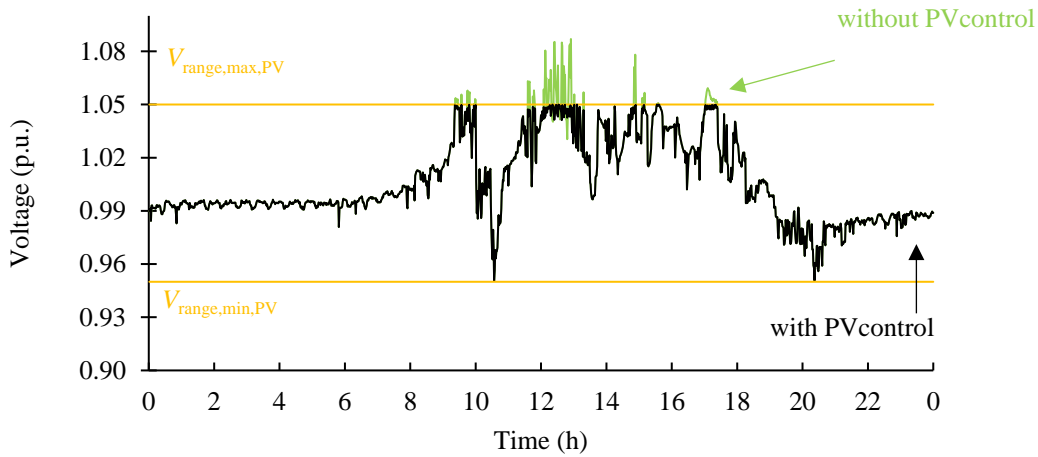


Fig. 6. Example of daily voltage profile: no control vs. reactive power from PV inverters - CONF#1, day#1, node #18.

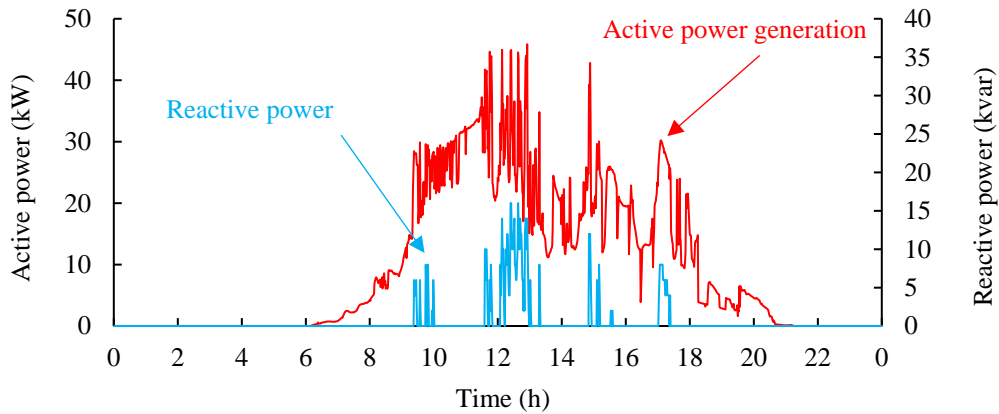


Fig. 7. Active and reactive profiles related to the example in Fig. 6.

Fig. 8 shows another voltage profile calculated in case of voltage control performed from both PV generators and the OLTC (Grid#1, day#2, node #18). At hour 10:30, the load increases leading to an undervoltage; the PV power production is still too low, and inverters do not

contribute with capacitive power. The load increase influences the voltage at the PCC of the OLTC (Fig. 9); it decreases the tap to adjust the voltage. After  $\approx 45$  min, the OLTC returns to the previous position. After midday, the overvoltages are managed by the PV inverters, with no other tap changes.

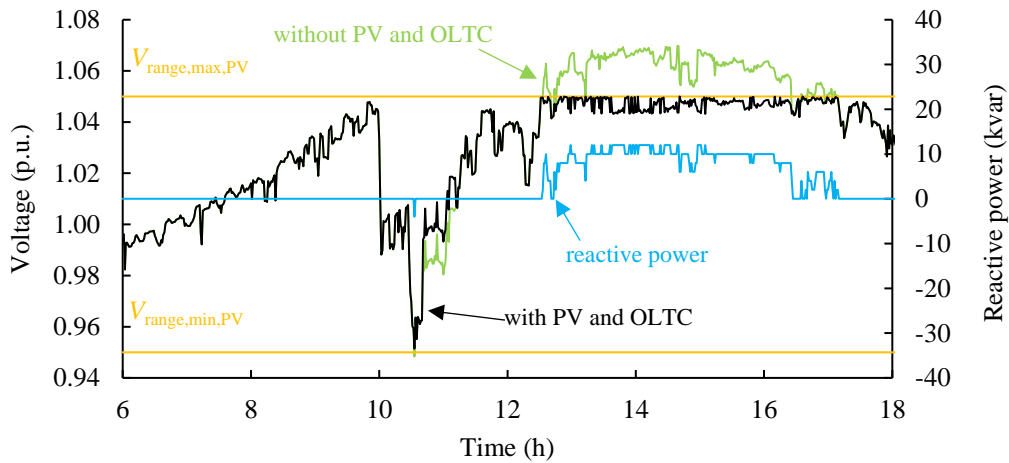


Fig. 8. Example of daily voltage profile: no control vs. OLTC+PV operation - CONF#1, day#2, node #18.

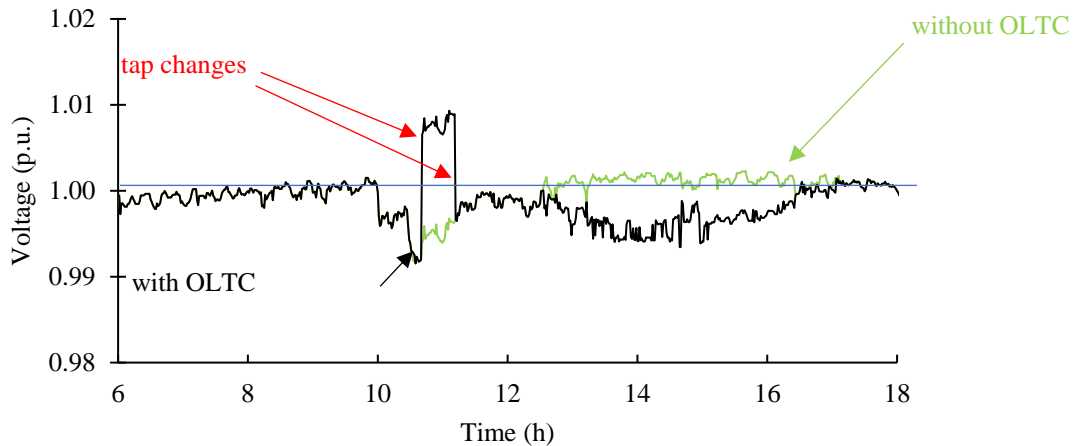


Fig. 9. OLTC operation related to the example in Fig. 8 - CONF#1, day#2, node #1 (LV side of the transformer).

Table 2 shows the values of the three objective functions  $VDEF$ ,  $L_{tot}$  and  $N_{tap}$  in case of voltage control performed by PV inverters, with or without OLTC operation. All the results refer to the whole week under analysis. In Grid#1, the  $VDEF$  decreases from  $2.99 \cdot 10^{-4}$  to  $2.90 \cdot 10^{-4}$  ( $\approx 5\%$ ) due to 8 tap changes. In Grid #2, the  $VDEF$  decreases from  $1 \cdot 10^{-4}$  to  $8.76 \cdot 10^{-5}$  due to 10 tap changes ( $\approx 15\%$ ). In both examples, the OLTC operation does not interfere with inverters



leading to higher losses  $L_{tot}$  (in Grid#1 the increment is negligible).

**Table 2. Losses and  $V_{def}$  with PV inverters or/and OLTC**

Grid	Objective function	Only PV inverters	PV inverters and OLTC
#1	$L_{tot}$ (kWh)	171	171
	$VDEF$	$2.99 \cdot 10^{-4}$	$2.90 \cdot 10^{-4}$
	$N_{tap}$ (phase 1)	-	8
#2	$L_{tot}$ (kWh)	54	54
	$VDEF$	$1 \cdot 10^{-4}$	$8.16 \cdot 10^{-5}$
	$N_{tap}$ (phase 1)	-	12

## 5.2 TOPSIS solutions ranking

The number of Scenarios (SC), simulated in the present work, is 1000 for each grid configuration, corresponding to a total of 6,000 scenarios. Each scenario starts with a different setup of the devices and includes a week of simulations with 1-min time step. For each grid configuration, the input parameters of voltage control devices are varied according to Section 3.2. Fig. 10 shows the Pareto front related to the three objective functions obtained in CONF#1. For the sake of simplicity, this figure does not show the third objective function  $L_{tot}$ . In the Pareto front there is a Scenario (SC#Φ) with minimum value of  $VDEF=1 \cdot 10^{-4}$ , while  $N_{tap} = 58$  and  $L_{tot} = 674$  kWh are not the lowest. This particular case has very high losses with respect to the average  $\approx 150$  kWh. Thus, a 3D view is necessary to better understand the scenario distribution. Fig. 11 shows the 3D Pareto front. The SCs are divided in three groups in the front, identified by three rectangles. One group is characterized by scenarios with higher voltage deviations and lower losses. In the other two groups,  $VDEF$  is lower due to higher use of reactive power, leading to high  $L_{tot}$ . In every group, the number of tap changes is quite variable, but in most cases is lower than 50.

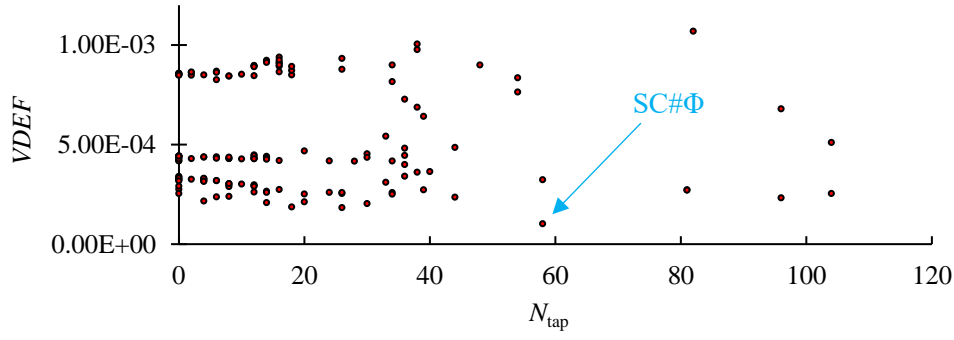


Fig. 10. Pareto front of two of the three objective functions – CONF#1.

After the calculation of the 149 non-dominated solutions, the TOPSIS method is applied, and the scenarios are ranked. In this case, the ranking weight for  $VDEF$  is  $w_{VDEF}=0.5$ , for the losses  $w_{L_{tot}}=0.4$ , and for the tap changes  $w_{N_{tap}}=0.1$ . Table 3 shows the resulting 5 best solutions.

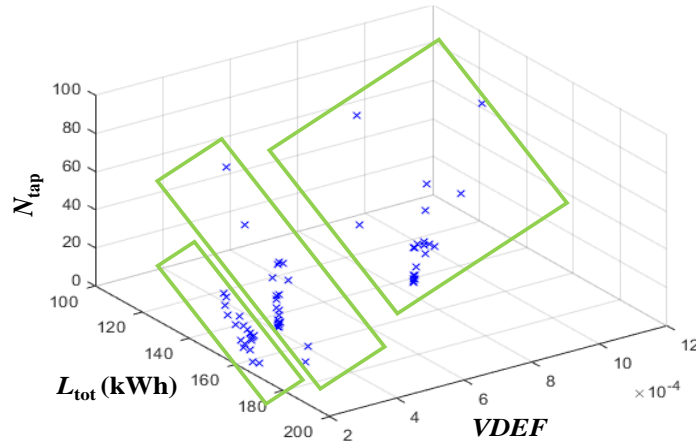


Fig. 11. 3D Pareto front of the three objective functions – CONF#1.

**Table 3. Best Solutions with  $w_{VDEF}=0.5$ ,  $w_{L_{tot}}=0.4$  and  $w_{N_{tap}}=0.1$  - Configuration#1**

Ranking	BS#1	BS#2	BS#3	BS#4	BS#5
$VDEF (\cdot 10^{-4})$	2.16	2.37	2.40	2.53	2.61
$L_{tot}$ (kWh)	165	161	156	162	151.3
$N_{tap}$	4	6	8	0	12
$V_{limit,max,PV}$ (p.u.)	1.075	1.094	1.085	1.085	1.098
$V_{limit,min,PV}$ (p.u.)	0.920	0.909	0.923	0.905	0.919
$V_{range,max,PV}$ (p.u.)	1.072	1.092	1.075	1.056	1.065
$V_{range,min,PV}$ (p.u.)	0.986	0.982	0.981	0.975	0.972
$V_{target}$ (p.u.)	1.003	1.002	1.003	1.001	1.002
$t_{adm}$ (min)	29	14	19	30	13
$t_{min,two,taps}$ (min)	18	25	4	26	20
$\alpha_{reset}$	24	29	8	29	14

The Best Scenario BS#1 has minimum  $VDEF = 2.16 \cdot 10^{-4}$  and  $N_{tap} = 4$ . BS#2 has  $VDEF = 2.37 \cdot 10^{-4}$  and  $N_{tap} = 6$ . The other scenarios have similar results, with losses between 165 and

151 kWh. The main difference is in the number of tap changes; the OLTC responsivity is mainly influenced by  $t_{adm}$ . The key point is the setup of the inverters: the range  $V_{range,max,PV} - V_{limit,max,PV}$  is small to limit the losses in the overvoltage management. Due to the reduced undervoltage in the case studies, the  $V_{limit,min,PV} - V_{range,min,PV}$  range is wide because it is less important for the loss increase. By changing the importance of losses, and focusing on voltage quality, the operation of inverter is boosted with a new set of weights, where  $w_{VDEF}$  is dominant,  $w_{VDEF}=0.8$ ,  $w_{Ltot}=0.1$ , and  $w_{Ntap}=0.1$ ; the results are shown in Table 4. With this new set of weights, the range  $V_{range,max,PV} - V_{limit,max,PV}$  is always much higher than in Table 3. The OLTC operation increases the voltage quality, mainly due to low values of  $t_{adm}$ .

**Table 4. Best Solutions with  $w_{VDEF}=0.8$ ,  $w_{Ltot}=0.1$  and  $w_{Ntap}=0.1$ - Configuration#1**

Scenario Ranking	BS#1	BS#2	BS#3	BS#4	BS#5
$VDEF (\cdot 10^{-4})$	1.86	1.83	2.16	2.12	2.03
$L_{tot}$ (kWh)	234	227	165	188	190
$N_{tap}$	18	26	4	20	30
$V_{limit,max,PV}$ (p.u.)	1.082	1.080	1.075	1.077	1.071
$V_{limit,min,PV}$ (p.u.)	0.925	0.924	0.920	0.911	0.918
$V_{range,max,PV}$ (p.u.)	1.056	1.050	1.073	1.051	1.050
$V_{range,min,PV}$ (p.u.)	0.997	0.988	0.986	0.982	0.982
$V_{target}$ (p.u.)	0.998	1.003	1.003	1.002	1.004
$t_{adm}$ (min)	25	12	29	9	19
$t_{min,two,taps}$ (min)	30	27	18	3	15
$\alpha_{reset}$	16	21	24	3	3

### 5.3 TOPSIS best solution in different grid configurations

Table 5 shows the best solution obtained with TOPSIS for the different grid configurations. CONF#1 is not included in Table 5, because data are already BS#1 in Table 4. Again, the ranking weights are  $w_{VDEF}=0.8$ ,  $w_{Ltot}=0.1$  and  $w_{Ntap}=0.1$ .

**Table 5. TOPSIS Solution for Different Grid Configurations**

Configuration	#2	#3	#4	#5	#6
$VDEF (\cdot 10^{-4})$	2.00	2.23	5.32	4.52	1.01
$L_{tot}$ (kWh)	444.5	275.1	57.9	24.7	101.1
$N_{tap}$	18	16	6	8	2
$V_{limit,max,PV}$ (p.u.)	1.072	1.082	1.075	1.079	1.082
$V_{limit,min,PV}$ (p.u.)	0.920	0.925	0.920	0.924	0.925
$V_{range,max,PV}$ (p.u.)	1.021	1.056	1.073	1.058	1.095
$V_{range,min,PV}$ (p.u.)	0.966	0.997	0.986	0.917	0.914
$V_{target}$ (p.u.)	0.994	0.998	1.003	1.002	1.000

Configuration	#2	#3	#4	#5	#6
$t_{adm}$ (min)	20	25	29	6	21
$t_{min,two,taps}$ (min)	28	30	18	18	25
$\alpha_{reset}$	25	16	24	8	18

The best scenario in CONF#2 is particular, because the voltage target of the OLTC is generally  $\approx 1$ . In this case, the target is lower leading to a high number of tap changes and high use of reactive power with the highest losses. Accepting a worsening, CONF#3 (despite the high PV injections) permits lower losses. In both cases, the setup of the OLTC is not the most responsive, and the number of tap changes is always below 20. In Grid #2 (CONF#4, #5 and #6) the same considerations can be applied.

#### 5.4 Sensitivity analysis of the TOPSIS weights

Another sensitivity analysis has been carried out to analyze how the results change by using different weights for the objective functions. Table 6 shows the results for the best scenario obtained for each set of weights in CONF#1. The sets of weights WS#3 and WS#6 lead to the same best scenario with the lowest  $VDEF$ , because  $w_{VDEF}$  is high. Thus, voltage control is the most efficient with many tap changes and high reactive power and losses. On the contrary, WS#4, WS#7 and WS#10 do not involve OLTC operation, with lower voltage quality. The other sets are compromises, where the best solution should be selected by the grid management.

**Table 6. Sensitivity Analysis of TOPSIS Weights - CONF#1**

Weight Set	$w_{VDEF}$	$w_{L_{tot}}$	$w_{N_{tap}}$	$VDEF (\cdot 10^{-4})$	$L_{tot}$ (kWh)	$N_{tap}$
1	0.5	0.4	0.1	2.16	165	4
2	0.4	0.4	0.2	2.16	165	4
3	0.8	0.1	0.1	1.86	234	18
4	0.2	0.4	0.4	2.76	152	0
5	0.3	0.6	0.1	2.40	156	8
6	0.9	0.05	0.05	1.86	234	18
7	0.3	0.2	0.5	2.53	162	0
8	0.7	0.2	0.1	2.16	165	4
9	0.1	0.1	0.8	2.53	162	0
10	0.3	0.1	0.6	2.53	162	0

## 6. Conclusions

The present study of voltage control in LV grids, performed by distributed PV inverters and OLTC, aimed to find the optimal setups for their operation without any coordination, even though a unique setup does not exist. Nevertheless, thanks to the result of the present work, the Distribution System Operators are given reference values to decide the setup for the distributed inverters to decide, considering their specific technical and economical constraints, how to face voltage issues. The Distribution System Operators can stress the control setups to improve voltage as much as possible, leading to higher Joule losses and maintenance cost, with less issues for the users. On the contrary, they can use less strict voltage control to avoid excessive increase in the costs.

The simulation results show how PV inverters can improve the voltage at their PCC adjusting their reactive power. Nevertheless, in LV grids the effects are limited, as the grid is not very inductive. On the contrary, the OLTC strongly affects the whole grid, but it cannot solve local voltage violations. Indeed, since there is no method of communication with other nodes of the grid, the OLTC may correct the voltage only at its PCC, where the voltage variation is low. Nevertheless, as shown in this work, implicit cooperation without communication between the OLTC and distributed PV inverters can be useful. The inverters will carry out a “*first*” partial voltage control. Simulations have shown that inserting large voltage ranges (i.e.,  $V_{\text{limit,min,PV}} - V_{\text{range,min,PV}}$  and  $V_{\text{range,max,PV}} - V_{\text{limit,max,PV}}$ ) involves an important increase in reactive power and losses to obtain a benefit on voltage. A large range with  $V_{\text{range,max,PV}} = 1.05$  and  $V_{\text{limit,max,PV}} \approx 1.08$  generally leads to a large use of reactive power and many tap changes (an average of  $\approx 20$  taps/day) to improve voltage with a resulting average value of  $VDEF \approx 2.14 \cdot 10^{-4}$ . Thus, for an optimal compromise between losses, voltage violations and lifespan increase of the OLTC, the ranges should be limited. Thus, the OLTC should solve the most serious voltage violations working as a “*second*” voltage controller. A lower range with  $V_{\text{range,max,PV}} = 1.07$  and  $V_{\text{limit,max,PV}}$

$\approx 1.08$  lead to a lower use of reactive power, and less tap changes (an average of  $\approx 7$  taps/day) to improve voltage; as a result the quality of voltage profiles is lower, with an average value of  $VDEF \approx 1.83 \cdot 10^{-4}$ . With respect the previously mentioned larger range  $V_{range,max,PV} - V_{limit,max,PV}$ , there is a drop in voltage quality of about 20%. The control by inverter and OLTC leads to better results when values of  $t_{adm}$  and  $t_{min,two,taps}$  are smaller. In this way, the control is more responsive to voltage variations. Therefore, the number of tap changes increases, and voltage deviation is reduced. For local voltage problems not solved by the studied control devices, the voltage quality could be improved by decreasing the impedance up to their PCC. Moreover, the present work has presented the procedure used to obtain the above-described results, in different setup scenarios and grid configurations. For each configuration, the Pareto analysis provides the non-dominated solutions. A TOPSIS analysis is included in the procedure to rank the scenarios. Finally, sensitivity analysis has been executed to evaluate how the results change according to the weights assigned to each objective function.

## 7. References

1. O.S. Nduka, L.P. Kunjumuhammed, B.C. Pal, A. Majumdar, Y. Yu, S. Maiti, A.R. Ahmad, Field Trial of Coordinated Control of PV and Energy Storage Units and Analysis of Power Quality Measurements, *IEEE Access*, vol. 8, pp. 1962–1974, 2020.
2. M. Pau, E. De Din, F. Ponci, P.A. Pegoraro, S. Sulis, C. Muscas, Impact of uncertainty sources on the voltage control of active distribution grids, *2021 International Conference on Smart Energy Systems and Technologies (SEST)*, pp. 1-6, 2021.
3. D. Zhang, J. Li, D. Hui, Coordinated Control for Voltage Control of Distribution Network Voltage Control by Distributed Energy Storage Systems, *Prot. and Contr. of Mod. Pow. Sys.*, vol. 3(1), pp. 1–8, 2018.
4. L. Del Rio Etayo, P. Cirujano, P. Lauzevis, G. Perez De Nalclares, A. Soto, A. Ulasenka, A new smart distribution transformer with OLTC for low carbon technologies integration, *24<sup>th</sup> Int. Conf. on Electricity Distribution*, paper no. 0832, Glasgow (UK), 12-15 June 2017.
5. A. Selim, M. Abdel-Akher, M.M. Aly, S. Kamel, T. Senjyu, Fast Quasi-static Time-series Analysis and Reactive Power Control of Unbalanced Distribution Systems, *International Transactions on Electrical Energy Systems*, vol. 29(1), ref. E2673, 2019.

6. M. Chamana, B.H. Chowdhury, F. Jahanbakhsh, Distributed Control of Voltage Regulating Devices in the Presence of High PV Penetration to Mitigate Ramp-Rate Issues, *IEEE Trans. on Smart Grid*, vol. 9(2), pp. 1086–1095, 2018.
7. N. Daratha, B. Das, J. Sharma, Coordination Between OLTC and SVC for Voltage Control in Unbalanced Distribution System Distributed Generation, *IEEE Trans. on Power Systems*, vol. 29(1), pp. 289–299, 2014.
8. J. Ma, H. Ye, L. Haifeng, Z. Li, P. Han, Z. Lin, J. Shi, Research on Source-Network Coordination Voltage Control Strategy of Photovoltaic Power Plant Considering the Stability of Inverter Port Voltage, *E3S Web of Conferences*, vol. 143, ref. 2018, 2020.
9. E.M. Darwish, H.M. Hasanien, A. Atallah, S. El-Debeiky, Reactive Power Control of Three-phase Low Voltage System Based on Voltage to Increase PV Penetration Levels, *Ain Shams Engineering Journal*, vol. 9(4), pp. 1831–1837, 2018.
10. V.B. Pamshetti, S.P. Singh, Optimal Coordination of PV Smart Inverter and Traditional Volt-VAR Control Devices for Energy Cost Savings and Voltage Control, *International Transactions on Electrical Energy Systems*, vol. 29(7), 2019.
11. M. Chamana and B.H. Chowdhury, Optimal Voltage Control of Distribution Networks With Cascaded Voltage Regulators in the Presence of High PV Penetration, *IEEE Trans. on Sustainable Energy*, vol. 9(3), pp. 1427–1436, 2018.
12. R. Tonkoski, L.A.C. Lopes, T.H.M. El-Fouly, Droop-based Active Power Curtailment for Overvoltage Prevention in Grid Connected PV Inverters, *2010 IEEE Int. Symp. on Industrial Electronics*, pp. 2388–2393, 2010.
13. S. M. Rostami, M. Hamzeh, Reactive Power Management of PV Systems by Distributed Cooperative Control in Low Voltage Distribution Networks, *2021 29th Iranian Conference on Electrical Engineering (ICEE)*, 2021, pp. 412–417.
14. A.M. Howlader, S. Sadoyama, L.R. Roose, S. Sepasi, Distributed voltage control using Volt-Var controls of a smart PV inverter in a smart grid: experimental study, *Renew. Energy*, vol. 127, pp. 145–157, 2018.
15. A.M. Howlader, S. Sadoyama, L.R. Roose, S. Sepasi, Distributed Voltage Control Method Using Volt-Var Control Curve of Photovoltaic Inverter for a Smart Power Grid System, *2017 IEEE 12th Int. Conf. on Power Electronics and Drive Systems (PEDS)*, pp. 630–634, 2017.
16. Z. Zhang, Y. Mishra, C. Dou, D. Yue, B. Zhang, Y.C. Tian, Steady-State Voltage Control With Reduced Photovoltaic Power Curtailment, *IEEE Journal of Photovoltaics*, vol. 10(6), pp. 1853–1863, 2020.
17. S. Wang, L. Du, X. Fan, Q. Huang, Deep Reinforcement Scheduling of Energy Storage Systems for Real-Time Voltage Regulation in Unbalanced LV Networks With High PV Penetration, *IEEE Trans. on Sustainable Energy*, vol. 12, no. 4, pp. 2342–2352, Oct. 2021.
18. F. Marra, G. Yang, C. Traeholt, J. Ostergaard, E. Larsen, A Decentralized Storage Strategy for Residential Feeders With Photovoltaics, *IEEE Trans. on Smart Grid*, vol. 5, pp. 974–981, 2014.
19. M.N. Kabir, Y. Mishra, G. Ledwich, Z.Y. Dong, K.P. Wong, Coordinated Control of Grid-Connected Photovoltaic Reactive Power and Battery Energy Storage Systems to Improve the Voltage Profile of a Residential Distribution Feeder, *IEEE Trans. on Industrial Informatics*, vol. 10(2), 967–977, 2014.

20. N. Efkarpidis, T. De Rybel, J. Driesen, Optimization control scheme utilizing small-scale distributed generators and OLTC distribution transformers, *Sustainable Energy, Grids and Networks*, vol. 8, pp. 74–84, 2016.
21. A. Ciocia, G. Chicco, F. Spertino, Benefits of On-Load Tap Changers Coordinated Operation for Voltage Control in Low Voltage Grids with High Photovoltaic Penetration, *2020 International Conference on Smart Energy Systems and Technologies (SEST)*, 2020.
22. D.G. Infield, M. Thomson, Network power-flow analysis for a high penetration of distributed generation, *2006 IEEE PES General Meeting*, 2006.
23. J. Wang, X. Zhu, D. Lubkeman, N. Lu, N. Samaan, B. Werts, Load Aggregation Methods for Quasi-Static Power Flow Analysis on High PV Penetration Feeders, *2018 IEEE/PES Transmission and Distribution Conference and Exposition (T&D)*, pp. 1-5, 2018.
24. M. de Montigny et al., Multiagent Stochastic Simulation of Minute-to-Minute Grid Operations and Control to Integrate Wind Generation Under AC Power Flow Constraints, *IEEE Trans. on Sustainable Energy*, vol. 4(3), pp. 619-629, 2013.
25. C. Plath, M. Putter, OMICRON electronics GmbH, Dynamic analysis and testing of On-Load Tap Changer with dynamic resistance measurement, Available online (accessed 31 March 2022): <https://www.omicronenergy.com/download/file/a207466e7bc405ecd22dbec942a41199/>
26. G.R. Chandra Mouli, P. Bauer, T. Wijekoon, A. Panosyan, E. Bärthlein, Design of a Power-Electronic-Assisted OLTC for Grid Voltage Regulation, *IEEE Trans. on Power Delivery*, vol. 30(3), pp. 1086-1095, 2015.
27. D. Dohnal, On-load tap-changers for power transformers, Available online (accessed 31 March 2022): [https://www.reinhausen.com/fileadmin/downloadcenter/company/publikationen/f0126405\\_on-load\\_tap-changers\\_for\\_power\\_transformers.pdf](https://www.reinhausen.com/fileadmin/downloadcenter/company/publikationen/f0126405_on-load_tap-changers_for_power_transformers.pdf)
28. D. Shirmohammadi, H.W. Hong, A. Semlyen, G.X. Luo, A Compensation-based Power Flow Method for Weakly Meshed Distribution and Transmission Networks, *IEEE Trans. on Power Systems*, vol. 3(2), pp. 753–762, 1988.
29. A. Ciocia, V.A. Boicea, G. Chicco, P. Di Leo, A. Mazza, E. Pons, F. Spertino, N. Hadj-Said, Voltage Control in Low-Voltage Grids Using Distributed Photovoltaic Converters and Centralized Devices, *IEEE Trans. on Industry Applications*, vol. 55(1), pp. 225–237, 2019.
30. Italian Electrotechnical Committee (CEI), Reference technical rules for the connection of active and passive users to the LV electrical Utilities, CEI Standard 0-21, December 2012 (In Italian).
31. A. Molina-Garcia, R.A. Mastromauro, T. Garcia-Sanchez, S. Pugliese, M. Liserre, S. Stasi, Reactive Power Flow Control for PV Inverters Voltage Support in LV Distribution Networks, *IEEE Trans. on Smart Grid*, vol. 8(1), pp. 447–456, 2017.
32. L. Collins, J.K. Ward, Real and Reactive Power Control of Distributed PV Inverters for Overvoltage Prevention and Increased Renewable Generation Hosting Capacity, *Renewable Energy*, vol. 81 pp. 464–471, 2015.
33. A.F. Murtaza, M. Chiaberge, F. Spertino, U. T. Shami, D. Boero, M. De Giuseppe, MPPT technique based on improved evaluation of photovoltaic parameters for uniformly irradiated photovoltaic array, *Electric Power Systems Research*, vol. 145, pp. 248-263, 2017.



34. F. Spertino, J. Ahmad, A. Ciocia, P. Di Leo, A technique for tracking the global maximum power point of photovoltaic arrays under partial shading conditions, *2015 IEEE 6th International Symposium on Power Electronics for Distributed Generation Systems (PEDG)*, pp. 1-5, 2015.
35. D. Zeng, J. Guo, M. Ding, D. Geng, Fault ride-through capability enhancement by adaptive voltage support control for inverter interfaced distributed generation, *2015 5th International Conference on Electric Utility Deregulation and Restructuring and Power Technologies (DRPT)*, pp. 1924-1928, 2015.
36. D. Iioka, H. Saitoh, Enhancement of fault ride through capability using constant current control of photovoltaic inverters, *2016 IEEE Innovative Smart Grid Technologies - Asia (ISGT-Asia)*, pp. 1083-1088, 2016.
37. E. Carpaneto, G. Chicco, M. De Donno, R. Napoli, Voltage controllability of distribution systems with local generation sources, *Bulk Power System Dynamics and Control*, Cortina d'Ampezzo, Italy, August 22-27, 2004, pp. 261-273.
38. A. Ciocia, G. Chicco, P. Di Leo, M. Gai, A. Mazza, F. Spertino, N. Hadj-Said, Voltage control in low voltage grids: A comparison between the use of distributed photovoltaic converters or centralized devices, *Proc. 2017 IEEE IEEEIC / I&CPS Europe*, pp. 1-6.
39. D.L. Olson, Comparison of weights in TOPSIS models, *Math. Comput. Model.*, vol. 40, no. 7-8, pp. 721-727, 2004.
40. F. Spertino, A. Ciocia, P. Di Leo, R. Tommasini, I. Berardone, M. Corrado, A. Infuso, M. Paggi, A Power and Energy Procedure in Operating Photovoltaic Systems to Quantify the Losses According to the Causes, *Solar Energy*, vol. 118, pp. 313-326, 2015.